Open access • Journal Article • DOI:10.1088/0022-3727/44/25/255302

Structural and transport properties in alloyed Ti/Al Ohmic contacts formed on p-type Al-implanted 4H-SiC annealed at high temperature

A. Frazzetto, Filippo Giannazzo, R. Lo Nigro, Vito Raineri ...+1 more authors

Institutions: University of Catania

Published on: 29 Jun 2011 - Journal of Physics D (IOP Publishing)

Topics: Ohmic contact, Contact resistance, Sheet resistance, Microstructure and Annealing (metallurgy)

Structural and transport properties in alloyed Ti/Al Ohmic contacts formed on p-type Al-implanted 4H-SiC annealed at high temperature

A Frazzetto, F Giannazzo, R Lo Nigro, V Raineri, F Roccaforte

Structural and transport properties in alloyed Ti/Al Ohmic contacts formed on p-type Al-implanted 4H-SiC annealed at high temperature

A. Frazzetto[1,2], F. Giannazzo [1], R. Lo Nigro [1], V. Raineri [1], F. Roccaforte [1]

[1] Consiglio Nazionale delle Ricerche – Istituto per la Microelettronica e Microsistemi (CNR-IMM) - Strada VIII n. 5, Zona Industriale, 95121, Catania, Italy
[2] Scuola Superiore di Catania – Università degli Studi di Catania - Via Valdisavoia, 9 – 95123 Catania, Italy

E-mail: alessia.frazzetto@imm.cnr.it, filippo.giannazzo@imm.cnr.it, raffaella.lonigro@imm.cnr.it, vito.raineri@imm.cnr.it, fabrizio.roccaforte@imm.cnr.it

Abstract. In this paper, the transport properties of alloyed Ti/Al Ohmic contacts formed on p-type Al-implanted silicon carbide (4H-SiC) were studied. The morphology of p-type implanted 4H-SiC was controlled by using a capping layer during post-implantation activation annealing at 1700°C. The different morphological conditions does not affect the macroscopic electrical properties of the implanted SiC (like the sheet resistance or the mobility). On the other hand, the improved morphology of implanted SiC allows to achieve a flatter Ti/Al surface and a lower specific contact resistance. The temperature dependence of the specific resistance of the contacts was studied to get physical insights into the carrier transport mechanism at the metal/SiC interface. The fit comparing several models shows that thermionic field emission is the dominant transport mechanism through the metal/SiC interface, and that a reduction of the barrier height from 0.51eV to 0.46 eV is associated to the improvement of the Ohmic properties. Transmission Electron Microscopy analysis showed the presence of a laterally inhomogeneous microstructure of the metal/SiC interface. The reduction of the barrier height could be correlated with the different microstructure of the interfacial region.
PACS.: 73.40.-c; 73.40.Cg; 73.40.Ns

Keywords: 4H-SiC, Ohmic contacts, Ti/Al, TLM, ion-implantation.

1. Introduction

Due to its excellent physical properties (like a wide band-gap, a high critical field, and a high thermal conductivity), silicon carbide (SiC) is today considered among the most promising materials for the new generation of power electronic devices with high performances, ensuring high-power and high-temperature operation and a significantly improved energy efficiency [1,2].
Ion-implantation is the method of choice used for local doping of SiC [1,3,4,5], since conventional diffusion techniques cannot be used, due to the small diffusivity of impurities in the material. As a matter of fact, ion-implantation doping of SiC is currently employed to fabricate several planar devices, like Schottky diodes, junction barrier Schottky (JBS) or metal-oxide-semiconductors field effect transistors (MOSFETs). However, in spite of the important and original progresses achieved in the last years, two closely linked physical issues still represent a concern for these devices, i.e., the p-type doping process by ion-implantation and the formation of Ohmic contacts on the implanted p-type regions. In particular, the reduction of the specific resistance of Ohmic contacts is required to minimize the total device series resistance (R_{ON}) and, ultimately, to reduce the overall power dissipation of single devices and/or complex power modules.

While for n-type doping of SiC an almost complete electrical activation of the implanted dopant with Phosphorous ions can be achieved already upon annealing at 1500°C [4,6], Aluminium (Al) implantation for p-type doping, requires annealing at higher temperatures (T = 1500-1800°C) to promote the electrical activation of the dopant in substitutional lattice sites [4,7,8,9]. However, efficient p-type doping by Al-

implantation remains a challenging task, due both the high ionization energies of acceptors, and to the high thermal budget required to achieve the electrical activation of the implanted dopants and remove the lattice damage [1, 2].

It is well known that the surface morphology of SiC can be strongly modified by the high thermal budgets necessary for the electrical activation of implanted dopants [10]. At high temperatures (~ 1500 °C) preferential evaporation of Si from the surface starts to occur, giving rise to a peculiar roughening of the surface, with the formation of large terraces parallel to the original miscut angle ("step bunching"). This step bunching is greatly enhanced in the regions subjected to high implantation doses [11,12], and could affect the transport properties in the material and/or, the electrical characteristics of metallic contacts formed on these implanted regions. In order to reduce this detrimental effect, the surface of SiC can be protected during post-implantation annealing by using a capping layer, mostly a carbon capping layer formed by a pyrolyzed photoresist film, which is then removed after annealing and before any other processing step of the wafer [13,14].

Although a variety of metals have been used to form Ohmic contacts to p-type SiC, metallization schemes based on Ti-Al layers have given the most promising results in terms of specific contact resistance both on epitaxial and implanted layers [15,16,17,18,19]. However, while most of these studies were focused on epitaxial p-type SiC layers, the impact of the surface morphology of implanted SiC (which in turn is influenced by the post-implantation annealing conditions during devices fabrication) on the properties of Ti/Al Ohmic contacts was not fully addressed so far. In few cases a homogenous interface could be obtained and a carrier transport mechanism was proposed [20].

In this paper, the morphology, microstructure and carrier transport mechanism in alloyed Ti/Al Ohmic contacts to p-type Al-implanted 4H-SiC were studied. In particular, it will be shown that the Al/Ti/SiC interface is not uniform on implanted 4H-SiC. An improvement of the SiC surface morphology before metal deposition can be achieved and it leads to a reduction of the Ti/Al roughness and of the specific contact resistance of the annealed Ti/Al Ohmic contacts. Combining temperature dependent electrical measurements with a microstructural analysis of the interfacial region allowed us to model the electrical behavior of the non uniform contacts.

2. Experimental Details

N-Type 4H-SiC epitaxial layers, 6μm-thick with a doping concentration of 1×10^{16} cm^{-3}, grown on heavily doped n^+-type substrates, were used in this work. The samples were implanted with Al-ions at 400 °C, using multiple energies (30-80 keV) at two different doses of $1.3\times10^{14}cm^{-2}$ and $1.3\times10^{15}cm^{-2}$ to form an almost uniform dopant profile extending over a depth of approximately 175 nm. Al-ion implantation was performed in selected regions, defined by a lithographic process. Post–implantation annealing at 1700 °C was carried out for electrical activation of the dopant, *with* and *without* a protective carbon capping layer, previously formed on the sample surface by a spinned layer of photoresist. The capping layer was removed after the high-temperature activation annealing, by a low temperature oxidation followed by an wet chemical cleaning. Ohmic contacts were formed by sputtering Ti(100nm)/Al(300nm) bi-layers on the p-type Al-implanted regions, followed by a rapid annealing at 950 °C in Ar for 60s. As previously reported by other authors [15,21,22], a different Ti/Al ratio can lead led to remarkable differences in elemental distribution, interface chemistry, surface roughness and reproducibility of Ti/Al Ohmic contacts to p-type SiC. Hence, in the present work the thickness of the metal layers was chosen basing on the common evidence, that an Al-rich condition is essential to yield low contact resistance in alloyed Ti/Al systems [15,23].

Linear transmission line model (TLM) [24] structures were fabricated for the macroscopic electrical characterization of both the p-type doped material and the Ohmic contacts, to determine the sheet resistance R_{SH} and specific contact resistance ρ_c. The TLM structures were defined by optical lithography and sequential wet etch of the two metal layers.

Current voltage (I-V) measurements were carried out using a four points probe station equipped with a HP 4156B parameter analyzer. The measurement temperature was varied in the range of 25–150 °C, using a Lakeshore 331 temperature controller connected to the chuck.

The surface morphology and the microstructure of both Ohmic contacts and implanted layers were investigated employing several techniques, including atomic force microscopy (AFM), transmission electron microscopy (TEM), and X-ray diffraction (XRD).

3. Result and Discussion

3.1 Surface morphology of implanted 4H-SiC and Ti/Al Ohmic contacts

The surface morphology of the Al-implanted 4H-SiC regions and of the Ti/Al Ohmic contacts were monitored by AFM before and after any treatment.

After Al-implantation at high dose ($1.3\times10^{15}cm^{-2}$), but before the post-implantation annealing at 1700°C, the samples exhibited a quite flat surface with a mean surface roughness (root mean square, RMS) of 1.14 nm; this RMS value is slightly increased with respect to the RMS of the as-grown material (0.9 nm). A similar behaviour was observed in the sample implanted at low dose ($1.3\times10^{14}cm^{-2}$).

Important changes of the RMS were observed after high temperature post-implantation annealing. Figures 1a and 1b show the AFM scans taken over 20×20 μm^2, for the samples implanted at high dose and annealed at 1700°C, either *without* or *with* the protective carbon capping layer. The scans were acquired after removal of the capping layer. As can be observed, the RMS of the samples has increased after high-temperature annealing. However, while the sample annealed without capping layer shows a significant increase of the RMS up to a value of 18.9 nm and a pronounced "step bunching" is present on the sample surface (figure 1a), the morphology of the sample annealed with the capping layer remained quite well preserved, with RMS value of 2.4 nm (figure 1b).

After high-temperature activation annealing at 1700°C and removal of the capping layer, Ti/Al bi-layers were sputtered on the 4H-SiC surface. Hence, rapid annealing at 950°C was carried out to achieve Ohmic characteristics of the contacts. The surface morphology of the annealed contacts is shown in figures 1c and 1d (for the contacts formed on SiC samples annealed *without* and *with* capping layer, respectively). It is evident that the alloyed Ti/Al contacts exhibit a large surface roughness, which is clearly influenced by the large RMS of the underlying implanted SiC. In fact, it can be noticed that the higher is the roughness of SiC, the higher the roughness of the alloyed Ti/Al contacts formed on it is. The RMS values of the contacts formed on the sample implanted at high dose were 44.0 nm and 22.8 nm, *without* and *with* the use of capping layer, respectively. A similar RMS trend was observed also in the case of low dose implantation. The results of the morphological AFM analysis, both for the SiC surface and Ti/Al Ohmic contacts, are summarized in Table 1. Clearly, the significant reduction of the surface roughness of the contacts can represent an advantage during SiC device fabrication, especially when the lithographic definition of critical geometries is required.

3.2 Specific contact resistance of Ti/Al Ohmic contacts

The macroscopic electrical properties of the contacts, evaluated by conventional TLM analysis carrier out at room temperature, showed a different electrical behaviour of the alloyed Ti/Al Ohmic contacts, depending on whether the capping layer was used or not. The results of TLM analysis are summarized in Table 2. The reported values are the average of several measurements performed on 10 different patterns fabricated in various regions of the sample surface.

In particular, Ti/Al contacts formed on the capped sample exhibit, on average, a lower specific contact resistance with respect to those formed on the uncapped sample. As an example, for the samples implanted at high dose specific contact resistance values of $\rho_c = 1.45\times10^{-4}\ \Omega cm^2$ and $\rho_c = 3.51\times10^{-4}\ \Omega cm^2$ were measured for the capped and uncapped sample, respectively. On the other hand, for the low implantated dose $\rho_c = 7.52\times10^{-4}\ \Omega cm^2$ and $\rho_c = 3.70\times10^{-3}\ \Omega cm^2$, for the capped and uncapped sample, respectively. Beside the practical advantage coming from the reduction of contact roughness, mentioned in the last paragraph, other important implications are related to the reduction of the specific contact resistance. In particular, considering that such such Ti/Al alloyed contacts can be used as metallization to p-type SiC in implanted p-n junctions or can be integrated in more complex devices (like JBS or MOSFETs), it is possible to estimate the impact of the reduction of ρ_c on the total specific series resistance R_{ON} of the p-n diode. Taking into account the different contributions to the series resistance (like the specific contact resistance ρ_c, the resistance of the p-type Al-implanted layer, and the contribution of the n-type epitaxial layer and substrate [25]), the experimentally observed reduction of ρ_c achieved when using a capping layer should result into an overall reduction of R_{ON} between 12 and 60%, depending on the implanted dose. This latter, in turn, can consequently lead to a reduction of the power dissipation or can give the possibility to reduce device area.

Higher values of ρ_c (ranging from 8×10^{-4} Ωcm^2 to 2×10^{-3} Ωcm^2) were reported by Ito *et al.* [26] for alloyed Ti/Al contacts formed on p-type 4H-SiC, doped by ion-implantation with a similar Al-concentration (~1×10^{19} cm^{-3}). The experimental values of ρ_c determined by the TLM showed a dispersion in the order of 20%. This latter could be ascribed to the electrical inhomogeneity of the metal/SiC interfacial region, as will be also demonstrated by a structural analysis in the paragraph 3.4. A similar spread in the values of ρ_c in Ti/Al alloyed contacts on p-type ion implanted 6H-SiC was also found by Moscatelli *et al.* [18], who pointed out that the specific contact resistance is expected to be highly sensitive even to small variations of the doping concentration.

Clearly, our results demonstrate that the electrical properties of alloyed Ti/Al Ohmic contacts can be improved when the contacts are formed on smoother SiC surfaces. Similarly, it was recently reported that the improved morphology of SiC surfaces, achieved using a protective graphite disk during the post-implantation annealing, leads to an improvement of the specific contact resistance ρ_c and uniformity also in the case of Ti/AlNi/W contacts [27]. However, an exhaustive explanation of this behaviour was not given in that work.

One could simply correlate the improvement of the specific contact resistance observed when using a capping layer to the better surface morphology of the alloyed Ti/Al bi-layer observed by AFM (figures 1c and 1d). However, the transport properties of the annealed Al/Ti/SiC system are related, to a large extent, to the nanoscale electro-structural properties of the interfacial region, including both the metal and the underlying implanted 4H-SiC. Hence, other experimental electrical and structural measurements (presented in the next paragraphs) were carried out in order to give a clearer physical scenario explaining our result.

3.3 Temperature dependence of the electrical properties of implanted 4H-SiC and Ti/Al Ohmic contacts

Firstly, the macroscopic electrical properties of the Al-implanted 4H-SiC (averaged over the entire implanted thickness) were monitored by means of both TLM analysis and room temperature Hall measurements.

The values of the sheet resistance R_{SH} of the implanted layer, determined by TLM analysis, are reported in Table 2. As can be seen, R_{SH} did not significantly depend on the use of the capping layer during high-temperature activation annealing, but it mainly depends on the Al-implanted dose. In fact, in the samples implanted at high dose the sheet resistance was in the order of 25 kΩ/sqr, while in the samples implanted at low dose was in the range 76-80 kΩ/sqr.

Room temperature Hall measurements allowed to estimate the free hole concentration in the implanted layer. Assuming a uniformly implanted layer of thickness t_{imp} = 175 nm, free holes concentration values of 6.63×10^{17} cm^{-3} and of 6.42×10^{17} cm^{-3} were determined for the samples implanted at high dose and annealed with and without capping layer, respectively. On the other hand, in the samples implanted at low – dose hole concentration values of 1.01×10^{17} cm^{-3} and of 9.96×10^{16} cm^{-3} were found respectively for the samples annealed with and without capping layer. The values of the Hall mobility, determined using a Hall scattering factor of 0.8 [28], were in the order of 17 $cm^2V^{-1}s^{-1}$ and 37 $cm^2V^{-1}s^{-1}$ for the high and the low implantation dose, respectively. Hence, as already observed for the sheet resistance, also the mobility is not influenced by the surface morphology.

The high values of sheet resistance and low free hole concentration determined at room temperature can be associated to an incomplete activation of the implanted Al dopant atoms. In fact, the free hole concentration p is only a small fraction of the implanted concentration, due to the high energy of the acceptor levels (~190 meV) [29] or to an incomplete activation of the implanted Al [30]. As a consequence, in some devices applications, like in the case of a JBS where p-type implanted stripes are integrated inside a n-type drift region, the high sheet resistance imposes a constraint in the layout, consisting in the need of a good Ohmic metallization over the entire stripe, in order to avoid any undesired potential drop and excess of series resistance under high current operation [3].

The sheet resistance R_{SH} of the implanted layer was determined by TLM analysis as a function of the temperature, performing TLM measurements varying the sample temperature between 25°C and 150°C. The results are shown in figure 2 for the sample implanted at high dose and annealed *with* or *without* the capping layer.

In both samples R_{SH} decreases in a similar way with increasing measurement temperature T, from around 25 kΩ/sqr at room temperature to 6.6 kΩ/sqr at 425 K.

For a uniformly implanted layer of thickness t_{imp}, the temperature dependent sheet resistance $R_{SH}(T)$ is related to the free hole concentration $p(T)$ and to the holes mobility $\mu_p(T)$ by the relation:

$$R_{SH}(T) = \frac{1}{q\mu_p(T)\,p(T)t_{imp}} \tag{1}$$

where q is the elementary charge.

For a p-type semiconductor the net free hole density $p(T)$ depends both on the acceptor concentration N_A and on the concentration of compensating donor centres N_D [31]. In particular, in the examined temperature range, the temperature dependence of free hole concentration $p(T)$ can be expressed by a simplified form [24,10].

$$p(T) \approx \frac{(N_A - N_D)N_V}{gN_D}\exp\left(-\frac{E_A}{kT}\right) \tag{2}$$

where N_V is the effective density of states in the valence band, g the degeneracy factor for acceptors (usually taken as 4), k is the Boltzmann constant, T the absolute temperature and E_A the ionization energy of acceptors referred to the top of the valence band.

The mobility μ_p depends both on N_A and on the temperature T. This dependence can be described by the following relation [32]:

$$\mu_p(T, N_A) = \mu_p(300, N_A)\left(\frac{T}{300}\right)^{-\beta(N_A)} \tag{3}$$

where $\mu_p(300, N_A)$ is the mobility at T=300 K and $\beta(N_A)$ is an empirical parameter which depends on the implanted doping concentration.

Hence, using the expression of N_V [24], the literature value $\beta(N_A) = 2.56$ for our doping conditions [32], and the experimental value of $\mu_p(300, N_A)$ determined by Hall measurements, it is possible to combine the Eqs. (2) and (3) with the expression of the sheet resistance (Eq. (1)), demonstrating that R_{SH} follows a thermally activated dependence as:

$$R_{SH} = T^{1.06}\frac{gN_D}{N_A - N_D}\frac{h^3}{2(2\pi m^*)^{3/2}}\frac{300^{-\beta}}{qt_{imp}\mu_p(300, N_A)}\exp\left(\frac{E_A}{kT}\right) \tag{4}$$

Hence, reporting in a semilogarithmic plot $\frac{R_{SH}}{T^{1.06}}$ as a function of the inverse of the absolute temperature should give an Arrhenius dependence, from which the activation energy can be determined.

Figure 3 reports the semilogarithmic plot of $\frac{R_{SH}}{T^{1.06}}$ as a function of q/kT, determined from the data in figure 2, for the samples implanted at high dose and annealed with and without capping layer. As it can be seen, the experimental data follows an Arrhenius law according to Eq. (4). From a linear fit, it was possible to determine the values of the activation energy E_A of 144 meV for the sample annealed with capping layer and 141 meV for the sample annealed without capping layer.

Clearly, all the electrical results presented above provided average information on the properties of the implanted layer (like the sheet resistance, free carrier concentration, mobility activation energy of the dopant), indicating that all these macroscopic quantities are not significantly affected by the surface morphology obtained in our conditions. However, in order to get further physical insights into the properties of Ohmic contacts, namely on the current transport at the Al/Ti/SiC interface, we monitored the temperature dependence of the specific contact resistance. In fact, in a metal/semiconductor system this dependence is typically related to fundamental physical parameters, like the barrier height Φ_B and the doping density N [33]. In particular, the barrier height is extremely sensitive to the interfacial properties (like the microstructure, presence of different phases, uniformity and surface inhomogeneity of the dopant activation). Such an analysis provided interesting information to understand the different electrical behaviour of the contacts fabricated on implanted SiC annealed with or without the capping layer.

The specific contact resistance ρ_c as a function of the temperature T, for the samples implanted at high-dose (with and without capping layer) is shown in figure 4. First of all, it can be observed that the values of ρ_c for the Ti/Al Ohmic contacts formed on 4H-SiC surfaces implanted and annealed with capping layer are lower that those measured in the samples without capping layer in the entire examined temperature range. Moreover, in both cases the specific contact resistance ρ_c decreases with increasing measuring

temperatures *T*. In particular, for Ti/Al contacts formed on capped 4H-SiC surface, ρ_c decreased from 1.45×10^{-4} Ωcm^2 at room temperature to 2.49×10^{-5} Ωcm^2 at 150°C. On the other hand, for the Ti/Al contact formed on the uncapped 4H-SiC ρ_c decreased from 3.51×10^{-4} Ωcm^2 to 9.69×10^{-5} Ωcm^2 in the same temperature range.

According to the classical treatment, the dominant carrier transport mechanism in metal/semiconductor interface depends on the doping density of the semiconductor *N*, and is related to a characteristics energy E_{00} defined by [34]:

$$E_{00} = \frac{h}{4\pi}\left(\frac{N}{m^*\varepsilon}\right)^{\frac{1}{2}} \tag{5}$$

where *h* is the Planck's constant, m^* is the hole effective mass and ε the dielectric permittivity of SiC.
E_{00} gives the relationship between the temperature *T* and the semiconductor net doping ($N = N_A - N_D$). The ratio kT/qE_{00} quantifies the ratio between the thermionic emission (TE) current and other contributions like the thermionic field emission (TFE) or the field emission (FE) one. A comparison of the thermal energy *kT* with E_{00} calculated for our doping levels and temperature range leads to $kT/qE_{00} \approx 0.86 - 1$. Hence, TFE can be assumed to be the dominant carrier transport mechanism.
According to the TFE model, the specific contact resistance can be expressed as [34,35]:

$$\rho_C = \left(\frac{1}{qA^*}\right)\frac{k^2}{\sqrt{\pi(\phi_B + V_n)E_{00}}}\cosh\left(\frac{E_{00}}{kT}\right)\times\left[\sqrt{\coth\left(\frac{E_{00}}{kT}\right)}\right]\exp\left(\frac{\phi_B + V_n}{E_0} - \frac{V_n}{kT}\right) \tag{6}$$

where

$$E_0 = E_{00}\coth\left(\frac{E_{00}}{kT}\right) \tag{7}$$

In Eq. (6) A^* is the Richardson constant and V_n the energy difference between the conduction band edge and the Fermi level.

The experimental data, reported in figure 4 were fitted using the expression of the TFE model, and the Schottky barrier height Φ_B and the doping concentration *N* were considered as fit parameters. Since the experimental results showed in the previous paragraph indicated that the average electrical properties of the implanted layer are almost independent on the use of the capping layer, a reasonable physical assumption is to consider the same value of *N* for both cases. Basing on this assumption, the experimental data for the two cases were fitted simultaneously, imposing the constrain of having the same parameter *N*.
For our calculation we used the values of $\varepsilon = 9.7\varepsilon_0$, ε_0 being the permittivity of free space, $A^* = 146$ A/cm^{2}K [36], and $m^* = 0.91\ m_0$ [37], with m_0 the electron mass.
For the sample annealed with capping layer a good fit of the experimental data was obtained using the TFE model, from which the values of $N=(2.0\pm0.1)\times10^{19}$ cm^{-3} and $\Phi_B=(0.46\pm0.01)$ eV were determined.
The value of *N* determined by the fit with the TFE model, that corresponds to an electrical activation of the dopant of around 20%, is in good agreement with previous experimental measurements of Al electrical activation in 4H-SiC obtained under similar doping conditions [38].
Few works reported the experimental values of the barrier height for Ti-Al based contacts to p-type implanted 4H-SiC, and these values critically depend on the contact formation conditions (e.g., metal thickness, deposition technique, doping and annealing conditions). As an example, using temperature dependent TLM measurements Scorzoni *et al*. [39] found a value of $\Phi_B=0.82$ eV on p-type ion implanted 4H-SiC for a doping concentration of 4×10^{19} cm^{-3}, while Crofton *et al.* [40] modeled the dependence of ρ_c on N_A assuming a barrier height of 0.37 eV. None of them, however, considered the incomplete activation of implanted Al.
By applying the TFE model considering the same doping concentration *N*, also for the sample annealed without capping layer, a higher Schottky barrier height ($\Phi_B=0.51\pm0.01$) eV was determined.
On the basis of this analysis, it can be concluded that TFE is the dominant transport mechanism in our Ti/Al Ohmic contacts. Furthermore, the reduction of the specific contact resistance, observed in the sample annealed with the capping layer, can be associated to a lowering of the Schottky barrier from 0.51 eV to 0.46 eV. However, it cannot be ruled out that local differences in the electrical activation of implanted Al-ions in the near-surface region occurring when using a capping layer, observed by scanning probe microscopy measurements in the absence of metal contacts [38], can play a role in the improvement of the values of ρ_c.

Furthermore, the deviations of the experimental data from model can be associated to the presence of an inhomogeneous metal–SiC interface, not considered in the classical TFE mechanism.

3.4 Microstructure of Ti/Al Ohmic contacts

In order to explain the different electrical behavior and to corroborate the information gained from the temperature dependence of ρ_c, the microstructure of the samples was evaluated by XRD analysis combined with cross-sectional TEM investigation.

Figure 5 shows XRD patterns of Ti/Al contact after annealing at 950 °C for the sample at high dose with capping layer. The main feature that can be deduced from the XRD patterns is the formation of a ternary compound Ti_3SiC_2 and of the Al_3Ti phase and the presence of unreacted Al. The same phases were observed in the sample annealed without capping layer (not shown). The phases observed by XRD in the alloyed contacts are in agreement with the predictions of the phase diagram of the Al-C-Ti-Si quaternary system, which indicates the coexistence of Ti_3SiC_2 and other compounds (like Al_4C_3 or Al_3Ti) upon annealing at 1000°C [41]. The presence of Al_4C_3, experimentally observed by Johnson et al [19], has not been detected in our samples, probably due to different annealing conditions.

Cross section TEM analysis, allowed the evaluation of contacts microstructure in the proximity of the interface, being relevant to understand the electrical properties determined by TLM analysis. Figures 6a and 6b show the cross sectional TEM micrographs for samples implanted at high dose and annealed at 1700°C without and with a capping layer, respectively. The combination of XRD (figure 5) and Energy Filtered TEM (EFTEM) analysis (this latter not shown in this paper), allowed to identify the elemental composition of the grains inside the reacted metal layer. The brighter regions in the TEM micrographs have been generically indicated as “Al-rich regions”, since the chemical analysis showed a predominance of Al, without the possibility to rule out the presence of small amount of Ti. Hence, according to the XRD analysis, inside these regions both pure Al and Al_3Ti may coexist. Furthermore, the ternary phase Ti_3SiC_2 is observed in both samples, resulting from the interaction of Ti with SiC at such high temperatures [41]. However, while in the sample without capping layer (figure 6a), large Ti_3SiC_2 grains are located close to the interface with SiC and interrupted by small Al-rich regions, in the sample with capping layer (figure 6b), larger Al-rich regions are found, in some parts forming an almost continous interfacial layer. Large agglomerates, already observed by AFM, were visible by TEM imaging in some places on the contact surface, and can be due to an excess of liquid Al freezed when cooling down the samples after annealing. Below the metal/SiC interface, a high density of extended defects can be observed, which was likely formed as a result the high dose implant followed by high temperature annealing. The presence of these defects is one of the causes of the high sheet resistance measured in the implanted material.

Evidently, TEM analysis showed a strongly inhomogeneous interface, where the interfacial morphology and microstructure are affected by the roughness of the implanted SiC. Although Ti was originally in contact with SiC, annealing of the contacts resulted in the formation of Ti_3SiC_2 interrupted by Al-rich regions. On the other hand, Tsukimoto *et al.* [23] found an irregular surface and interface morphology of the annealed Ti/Al system, attributing them to an anisotropic growth process of hetero-epitaxial Ti_3SiC_2 layers onto off-axis SiC layers. However, the ternary phase totally covered the area of the SiC substrate in their case. An inhomogeneous interfacial microstructure, similar to that of our samples, was found also by Parisini *et al.* [42], who detected the presence of titanium compounds and Al or Al_3Ti agglomerates, but did not report any correlation with the electrical measurements.

4. Summary

In summary, the carrier transport mechanism in alloyed Ti/Al Ohmic contacts to p-type Al-implanted 4H-SiC was modelled in this work considering transport mechanism at inomogeneous interfaces. It has been shown that the morphology of implanted SiC after high temperature (1700°C) annealing strongly influences both the surface flatness and the electrical characteristics of alloyed Al/Ti Ohmic contacts formed on it. In particular, improving the SiC surface morphology using a protective cap during post-implantation annealing resulted in a reduction of the roughness even if a uniform interface, similar to epitaxial substrates, cannot be achieved. Anyway a lowering of the specific resistance ρ_c of alloyed Ti/Al Ohmic contacts was achieved.This result could not be correlated to macroscopic electrical properties of the implanted layer, that

were independent on the surface conditions. However, the temperature dependence of the ρ_c indicated that thermionic field emission is the dominant transport mechanism through the metal/SiC interface, and that a reduction of the barrier height occurs in the contacts formed on smoother SiC surface and explains the lower specific contact resistance. As a matter of fact, TEM analysis shows an inhomogenous interface, different in the two cases, which can justify the different macroscopically measured Schottky barrier heights.

The practical implications of an improved Ohmic contact morphology and specific contact resistance, with respect to the possible applications to SiC device processing and performances were discussed.

Acknowledgements

The authors would like to thank L. Romano for help and discussion concerning Hall measurements, and K. Zekentes for the fruitful discussion during ECSCRM2010 in Oslo. C. Bongiorno and S. Di Franco are greatly acknowledged for TEM analysis and for samples processing, respectively.
This work was supported by ST Microelectronics of Catania and by the LAST POWER project. The LAST POWER project has received funding from the ENIAC Joint Undertaking under grant agreement n° 120218 and from the national programmes/funding authorities of Greece, Italy, Poland, and Sweden.

Table 1. Surface roughness (RMS) of 4H-SiC and alloyed Ti/Al contacts for the different implantation/annealing conditions.

	High – dose		**Low – dose**	
as–grown 4H-SiC	0.9 nm		0.9 nm	
as-implanted 4H-SiC	1.14 nm		1.10 nm	
	Without Cap	**With Cap**	**Without Cap**	**With Cap**
Implanted and annealed (1700°C) 4H–SiC	18.9 nm	2.4 nm	9.0 nm	1.3 nm
Alloyed (950°C) Ti/Al contacts	44.0 nm	22.8 nm	43.5 nm	20.8 nm

Table 2. Specific contact resistance ρ_c of alloyed Ti/Al contacts and sheet resistance R_{SH} of Al-implanted 4H-SiC measured at room temperature for the different implantation/annealing conditions.

	With cap		**Without cap**	
	High-dose	**Low-dose**	**High-dose**	**Low-dose**
$\rho_C(\Omega cm^2)$	1.45×10^{-4}	7.52×10^{-4}	3.51×10^{-4}	3.70×10^{-3}
$R_{SH}(\Omega/sqr)$	24.84×10^{3}	76.56×10^{3}	25.45×10^{3}	80.50×10^{3}

FIGURE CAPTIONS

Figure 1. AFM scans of Al-implanted 4H-SiC surface for samples implanted at high-dose and annealed at 1700°C without capping layer (a) and with capping layer (b). AFM scans of alloyed Ti/Al contacts formed on Al-implanted 4H-SiC surface for samples annealed without capping layer (c) and with capping layer (d).

Figure 2. Sheet resistance R_{SH} of implanted 4H-SiC as a function of the measurement temperature for the high implantation dose and annealing at 1700°C "with" and "without" capping layer.

Figure 3. Semilogarithmic plot of $\frac{R_{SH}}{T^{1.06}}$ as a function of *q/kT* for the samples implanted at high-dose and annealed at 1700°C "with" and "without" capping layer.

Figure 4. Specific contact resistance ρ_c as a function of the measurement temperature for alloyed Ti/Al contacts formed on 4H-SiC implanted at high-dose and annealed at 1700°C "with" and "without" capping layer. The fits obtained using TFE model for the both samples implanted at high dose and annealed at 1700 °C "with" and "without" protective capping layer are also reported.

Figure 5. XRD analysis of a Ti/Al contact after annealing at 950 °C formed on implanted 4H-SiC

Figure 6. Cross sectional TEM micrographs of the interfacial region for samples implanted at high dose and annealed at 1700°C "without" capping layer (a) and "with" capping layer (b).

References

[1] Pensl G, Ciobanu F, Frank T, Krieger M, Reshanov S, Schmid F and Weidner M 2006 *SiC Materials and Devices,* Shur M, Rumyanstev S and Levinshtein M eds., Singapore, World Scientific, Vol. 1, pag. 1-41.
[2] Roccaforte F, Giannazzo F, Raineri V 2010 *J. Phys. D: Appl. Phys.* **43** 223001.
[3] Baliga BJ 2005 *Silicon Carbide Power Devices*, Singapore, World Scientific.
[4] Mitra S, Rao M V, Papanicolaou N, Jones K A, Holland O W, Vispute R D, Wilson SR 2004 *J. Appl. Phys*. **95** 69.
[5] Roccaforte F, Libertino S, Giannazzo F, Bongiorno C, La Via F, Raineri V 2005 *J. Appl. Phys* **97** 123502.
[6] Laube M, Schmid F, Pensl G, Wagner G, Linnarsson M, Maier M 2002 *J. Appl. Phys.* **92** 549.
[7] Saks N S*,* Agarwal A K*,* Ryu S-H, and Palmour J W 2001 *J. Appl. Phys.* **90** 2796.
[8] Negoro Y, Kimoto T, Matsunami H, Schmid F and Pensl G 2004 *J. Appl. Phys.* **95** 4916.
[9] Sundaresan S G, et al., 2008 *Solid-State Electronics* **52** 140.
[10] Rambach M, Bauer A J, and Ryssel H 2008 *Phys. Stat. Sol. (b)* **245** (7) 1315.
[11] Brauer G, Anwand W, SkorupaW, Brandstetter S and Teichert C, 2006 *J. Appl. Phys.* **99** 023523.
[12] Giannazzo F, Rambach M, Salinas D, Roccaforte F and Raineri V 2009 *Mater. Sci. Forum* **615-617** 457.
[13] Vassilevski K V, Wright N G, Horsfall A B, O'Neill A G, Uren M J, Hilton K P, Masterton A G, Hydes A J and Johnson C M 2005 *Semicond. Sci. Technol*. **20** 271.
[14] Nipoti R, Mancarella F, Moscatelli F, Rizzoli R, Zampolli S, Ferri M 2010 *Electrochem. Solid-State Lett.* **13** H432.
[15] Crofton J, Money S E, Williams J R, Isaacs-Smith T 2002 *Solid-State Electronics* **46** 109.
[16] Roccaforte F, La Via F, Raineri V 2005 *Int. J. High Speed Electronics and Systems* **15** 781.
[17] Tsukimoto S, Sakai T, Onishi T, Ito K, and Murakami M, 2005 *J. Electronic Materials* **34** 1310.
[18] Moscatelli F, Scorzoni A, Poggi A, Cardinali GC, Nipoti R 2003 *Semicond. Sci. Technol.* **18** 554.
[19] Johnson B J, Capano M A 2004 *J. Appl. Phys.* **95** 5616.
[20] Wang Z, Saito M, Tsukimoto S, and Ikuhara Y 2009 *Advaced Materials* **21** 4966.
[21] Mohney S E, Hull B A, Lin J Y, Crofton J 2002 *Solid-State Electronics* **46** 689.
[22] Kolaklieva L, Kakanakov R, Avramova I, Marinova Ts 2007 *Mater. Sci. Forum* **556-557** 725.
[23] Tsukimoto S, Ito K, Wang Z, Saito M, Ikuhara Y, Murakami M 2009 *Materials Transactions* **50** 1071.
[24] Schroder D K 2006 *Semiconductors Materials and Device Characterization*, 3rd ed., New York, John Wiley & Sons, p. 135.
[25] La Via F, Galvagno G, Roccaforte F, Ruggiero A, Calcagno L, 2005 *Appl. Phys. Lett.* **87**, 142105.
[26] Ito K, Tsukimoto S, Murakami M 2006 *Science and Technology of Advanced Materials* **7** 496.
[27] Tsao B H, Liu S, Scofield J 2004 *Mater. Sci. Forum* **457-460** 841.
[28] Pensl G, Schmid F, Ciobanu F, Laube M, Reshanov S A, Schulze N, Semmelroth K, Nagasawa H, Schöner A, Wagner G 2003 *Mater. Sci. Forum* **433 – 436** 365.
[29] Pernot J, Contreras S, Camassel J 2005 *J. Appl. Phys.* **98** 023706.
[30] Giannazzo F, Roccaforte F, Raineri V 2007 *Appl. Phys. Lett.* **91** 202104.
[31] Sze S M, 2001 *Semiconductor Devices: Physics and Technology*, 2nd ed., New York, John Wiley & Sons Inc.
[32] Matsuura H, Komeda M, Kagamihara S, Iwata H, Ishihara R, Hatakeyama T, Watanabe T, Kojima K, Shinohe T, Arai K 2004 *J. Appl. Phys.,* **96** 2708.
[33] Iucolano F, Roccaforte F, Alberti A, Buongiorno C, Di Franco S, Raineri V 2006 *J. Appl. Phys.* **100** 123706.
[34] Padovani F A, Stratton R 1966 *Solid – State Electron* **9** 695.
[35] Yu A Y C 1970 *Solid-State Electronics* **13** 239.
[36] Roccaforte F, La Via F, Raineri V, Pierobon R, Zanoni E 2003 *J. Appl. Phys.* **93** 9137.
[37] Son N T, Hai P N, Chen W M, Hallin C, Monemar B, Janzén E 2000 *Phys. Rev. B* **61** R10544.
[38] Weng M H, Roccaforte F, Giannazzo F, Di Franco S, Bongiorno C, Saggio M, Raineri V 2010 *Mater. Sci. Forum* **645-648** 713.
[39] Scorzoni A, Moscatelli F, Poggi A, Cardinali G C, Nipoti R 2004 *Mater. Sci. Forum* **457-460** 881.
[40] Crofton J, Porter L M, Williams J R 1997 *Phys. Stat. Sol. (b)* **202** 549.
[41] Viala J C, Peillon N, Bosselet F, Bouix J 1997 *Mat. Sci. Eng.,* **A229** 95.
[42] Parisini A, Poggi A, Nipoti R 2004 *Mater. Sci. Forum* **457-460** 837.

Structural and transport properties in alloyed Ti/Al Ohmic contacts formed on p-type Al-implanted 4H-SiC annealed at high temperature

A. Frazzetto[1,2], F. Giannazzo [1], R. Lo Nigro [1], V. Raineri [1], F. Roccaforte [1]

[1] Consiglio Nazionale delle Ricerche – Istituto per la Microelettronica e Microsistemi (CNR-IMM) - Strada VIII n. 5, Zona Industriale, 95121, Catania, Italy
[2] Scuola Superiore di Catania – Università degli Studi di Catania - Via Valdisavoia, 9 – 95123 Catania, Italy

E-mail: alessia.frazzetto@imm.cnr.it, filippo.giannazzo@imm.cnr.it, raffaella.lonigro@imm.cnr.it, vito.raineri@imm.cnr.it, fabrizio.roccaforte@imm.cnr.it

Abstract. In this paper, the transport properties of alloyed Ti/Al Ohmic contacts formed on p-type Al-implanted silicon carbide (4H-SiC) were studied. The morphology of p-type implanted 4H-SiC was controlled by using a capping layer during post-implantation activation annealing at 1700°C. The different morphological conditions does not affect the macroscopic electrical properties of the implanted SiC (like the sheet resistance or the mobility). On the other hand, the improved morphology of implanted SiC allows to achieve a flatter Ti/Al surface and a lower specific contact resistance. The temperature dependence of the specific resistance of the contacts was studied to get physical insights into the carrier transport mechanism at the metal/SiC interface. The fit comparing several models shows that thermionic field emission is the dominant transport mechanism through the metal/SiC interface, and that a reduction of the barrier height from 0.51eV to 0.46 eV is associated to the improvement of the Ohmic properties. Transmission Electron Microscopy analysis showed the presence of a laterally inhomogeneous microstructure of the metal/SiC interface. The reduction of the barrier height could be correlated with the different microstructure of the interfacial region.
PACS.: 73.40.-c; 73.40.Cg; 73.40.Ns

Keywords: 4H-SiC, Ohmic contacts, Ti/Al, TLM, ion-implantation.

1. Introduction

Due to its excellent physical properties (like a wide band-gap, a high critical field, and a high thermal conductivity), silicon carbide (SiC) is today considered among the most promising materials for the new generation of power electronic devices with high performances, ensuring high-power and high-temperature operation and a significantly improved energy efficiency [1,2].
Ion-implantation is the method of choice used for local doping of SiC [1,3,4,5], since conventional diffusion techniques cannot be used, due to the small diffusivity of impurities in the material. As a matter of fact, ion-implantation doping of SiC is currently employed to fabricate several planar devices, like Schottky diodes, junction barrier Schottky (JBS) or metal-oxide-semiconductors field effect transistors (MOSFETs). However, in spite of the important and original progresses achieved in the last years, two closely linked physical issues still represent a concern for these devices, i.e., the p-type doping process by ion-implantation and the formation of Ohmic contacts on the implanted p-type regions. In particular, the reduction of the specific resistance of Ohmic contacts is required to minimize the total device series resistance (R_{ON}) and, ultimately, to reduce the overall power dissipation of single devices and/or complex power modules.

While for n-type doping of SiC an almost complete electrical activation of the implanted dopant with Phosphorous ions can be achieved already upon annealing at 1500°C [4,6], Aluminium (Al) implantation for p-type doping, requires annealing at higher temperatures (T = 1500-1800°C) to promote the electrical activation of the dopant in substitutional lattice sites [4,7,8,9]. However, efficient p-type doping by Al-

implantation remains a challenging task, due both the high ionization energies of acceptors, and to the high thermal budget required to achieve the electrical activation of the implanted dopants and remove the lattice damage [1, 2].

It is well known that the surface morphology of SiC can be strongly modified by the high thermal budgets necessary for the electrical activation of implanted dopants [13]. At high temperatures (~ 1500 °C) preferential evaporation of Si from the surface starts to occur, giving rise to a peculiar roughening of the surface, with the formation of large terraces parallel to the original miscut angle ("step bunching"). This step bunching is greatly enhanced in the regions subjected to high implantation doses [14,15], and could affect the transport properties in the material and/or, the electrical characteristics of metallic contacts formed on these implanted regions. In order to reduce this detrimental effect, the surface of SiC can be protected during post-implantation annealing by using a capping layer, mostly a carbon capping layer formed by a pyrolyzed photoresist film, which is then removed after annealing and before any other processing step of the wafer [16,17].

Although a variety of metals have been used to form Ohmic contacts to p-type SiC, metallization schemes based on Ti-Al layers have given the most promising results in terms of specific contact resistance both on epitaxial and implanted layers [18,19,20,21,22]. However, while most of these studies were focused on epitaxial p-type SiC layers, the impact of the surface morphology of implanted SiC (which in turn is influenced by the post-implantation annealing conditions during devices fabrication) on the properties of Ti/Al Ohmic contacts was not fully addressed so far. In few cases a homogenous interface could be obtained and a carrier transport mechanism was proposed [23].

In this paper, the morphology, microstructure and carrier transport mechanism in alloyed Ti/Al Ohmic contacts to p-type Al-implanted 4H-SiC were studied. In particular, it will be shown that the Al/Ti/SiC interface is not uniform on implanted 4H-SiC. An improvement of the SiC surface morphology before metal deposition can be achieved and it leads to a reduction of the Ti/Al roughness and of the specific contact resistance of the annealed Ti/Al Ohmic contacts. Combining temperature dependent electrical measurements with a microstructural analysis of the interfacial region allowed us to model the electrical behavior of the non uniform contacts.

2. Experimental Details

N-Type 4H-SiC epitaxial layers, 6μm-thick with a doping concentration of 1×10^{16} cm^{-3}, grown on heavily doped n^+-type substrates, were used in this work. The samples were implanted with Al-ions at 400 °C, using multiple energies (30-80 keV) at two different doses of $1.3\times10^{14}cm^{-2}$ and $1.3\times10^{15}cm^{-2}$ to form an almost uniform dopant profile extending over a depth of approximately 175 nm. Al-ion implantation was performed in selected regions, defined by a lithographic process. Post–implantation annealing at 1700 °C was carried out for electrical activation of the dopant, *with* and *without* a protective carbon capping layer, previously formed on the sample surface by a spinned layer of photoresist. The capping layer was removed after the high-temperature activation annealing, by a low temperature oxidation followed by an wet chemical cleaning. Ohmic contacts were formed by sputtering Ti(100nm)/Al(300nm) bi-layers on the p-type Al-implanted regions, followed by a rapid annealing at 950 °C in Ar for 60s. As previously reported by other authors [18,24,25], a different Ti/Al ratio can lead led to remarkable differences in elemental distribution, interface chemistry, surface roughness and reproducibility of Ti/Al Ohmic contacts to p-type SiC. Hence, in the present work the thickness of the metal layers was chosen basing on the common evidence, that an Al-rich condition is essential to yield low contact resistance in alloyed Ti/Al systems [18,26].

Linear transmission line model (TLM) [27] structures were fabricated for the macroscopic electrical characterization of both the p-type doped material and the Ohmic contacts, to determine the sheet resistance R_{SH} and specific contact resistance ρ_c. The TLM structures were defined by optical lithography and sequential wet etch of the two metal layers.

Current voltage (I-V) measurements were carried out using a four points probe station equipped with a HP 4156B parameter analyzer. The measurement temperature was varied in the range of 25–150 °C, using a Lakeshore 331 temperature controller connected to the chuck.

The surface morphology and the microstructure of both Ohmic contacts and implanted layers were investigated employing several techniques, including atomic force microscopy (AFM), transmission electron microscopy (TEM), and X-ray diffraction (XRD).

3. Result and Discussion

3.1 Surface morphology of implanted 4H-SiC and Ti/Al Ohmic contacts

The surface morphology of the Al-implanted 4H-SiC regions and of the Ti/Al Ohmic contacts were monitored by AFM before and after any treatment.

After Al-implantation at high dose ($1.3\times10^{15}cm^{-2}$), but before the post-implantation annealing at 1700°C, the samples exhibited a quite flat surface with a mean surface roughness (root mean square, RMS) of 1.14 nm; this RMS value is slightly increased with respect to the RMS of the as-grown material (0.9 nm). A similar behaviour was observed in the sample implanted at low dose ($1.3\times10^{14}cm^{-2}$).

Important changes of the RMS were observed after high temperature post-implantation annealing. Figures 1a and 1b show the AFM scans taken over 20×20 μm^2, for the samples implanted at high dose and annealed at 1700°C, either *without* or *with* the protective carbon capping layer. The scans were acquired after removal of the capping layer. As can be observed, the RMS of the samples has increased after high-temperature annealing. However, while the sample annealed without capping layer shows a significant increase of the RMS up to a value of 18.9 nm and a pronounced "step bunching" is present on the sample surface (figure 1a), the morphology of the sample annealed with the capping layer remained quite well preserved, with RMS value of 2.4 nm (figure 1b).

After high-temperature activation annealing at 1700°C and removal of the capping layer, Ti/Al bi-layers were sputtered on the 4H-SiC surface. Hence, rapid annealing at 950°C was carried out to achieve Ohmic characteristics of the contacts. The surface morphology of the annealed contacts is shown in figures 1c and 1d (for the contacts formed on SiC samples annealed *without* and *with* capping layer, respectively). It is evident that the alloyed Ti/Al contacts exhibit a large surface roughness, which is clearly influenced by the large RMS of the underlying implanted SiC. In fact, it can be noticed that the higher is the roughness of SiC, the higher the roughness of the alloyed Ti/Al contacts formed on it is. The RMS values of the contacts formed on the sample implanted at high dose were 44.0 nm and 22.8 nm, *without* and *with* the use of capping layer, respectively. A similar RMS trend was observed also in the case of low dose implantation. The results of the morphological AFM analysis, both for the SiC surface and Ti/Al Ohmic contacts, are summarized in Table 1. Clearly, the significant reduction of the surface roughness of the contacts can represent an advantage during SiC device fabrication, especially when the lithographic definition of critical geometries is required.

3.2 Specific contact resistance of Ti/Al Ohmic contacts

The macroscopic electrical properties of the contacts, evaluated by conventional TLM analysis carrier out at room temperature, showed a different electrical behaviour of the alloyed Ti/Al Ohmic contacts, depending on whether the capping layer was used or not. The results of TLM analysis are summarized in Table 2. The reported values are the average of several measurements performed on 10 different patterns fabricated in various regions of the sample surface.

In particular, Ti/Al contacts formed on the capped sample exhibit, on average, a lower specific contact resistance with respect to those formed on the uncapped sample. As an example, for the samples implanted at high dose specific contact resistance values of $\rho_c = 1.45\times10^{-4}\ \Omega cm^2$ and $\rho_c = 3.51\times10^{-4}\ \Omega cm^2$ were measured for the capped and uncapped sample, respectively. On the other hand, for the low implantated dose $\rho_c = 7.52\times10^{-4}\ \Omega cm^2$ and $\rho_c = 3.70\times10^{-3}\ \Omega cm^2$, for the capped and uncapped sample, respectively. Beside the practical advantage coming from the reduction of contact roughness, mentioned in the last paragraph, other important implications are related to the reduction of the specific contact resistance. In particular, considering that such such Ti/Al alloyed contacts can be used as metallization to p-type SiC in implanted p-n junctions or can be integrated in more complex devices (like JBS or MOSFETs), it is possible to estimate the impact of the reduction of ρ_c on the total specific series resistance R_{ON} of the p-n diode. Taking into account the different contributions to the series resistance (like the specific contact resistance ρ_c, the resistance of the p-type Al-implanted layer, and the contribution of the n-type epitaxial layer and substrate [28]), the experimentally observed reduction of ρ_c achieved when using a capping layer should result into an overall reduction of R_{ON} between 12 and 60%, depending on the implanted dose. This latter, in turn, can consequently lead to a reduction of the power dissipation or can give the possibility to reduce device area.

Higher values of ρ_c (ranging from 8×10^{-4} Ωcm^2 to 2×10^{-3} Ωcm^2) were reported by Ito *et al.* [29] for alloyed Ti/Al contacts formed on p-type 4H-SiC, doped by ion-implantation with a similar Al-concentration (~1×10^{19} cm^{-3}). The experimental values of ρ_c determined by the TLM showed a dispersion in the order of 20%. This latter could be ascribed to the electrical inhomogeneity of the metal/SiC interfacial region, as will be also demonstrated by a structural analysis in the paragraph 3.4. A similar spread in the values of ρ_c in Ti/Al alloyed contacts on p-type ion implanted 6H-SiC was also found by Moscatelli *et al.* [21], who pointed out that the specific contact resistance is expected to be highly sensitive even to small variations of the doping concentration.

Clearly, our results demonstrate that the electrical properties of alloyed Ti/Al Ohmic contacts can be improved when the contacts are formed on smoother SiC surfaces. Similarly, it was recently reported that the improved morphology of SiC surfaces, achieved using a protective graphite disk during the post-implantation annealing, leads to an improvement of the specific contact resistance ρ_c and uniformity also in the case of Ti/AlNi/W contacts [30]. However, an exhaustive explanation of this behaviour was not given in that work.

One could simply correlate the improvement of the specific contact resistance observed when using a capping layer to the better surface morphology of the alloyed Ti/Al bi-layer observed by AFM (figures 1c and 1d). However, the transport properties of the annealed Al/Ti/SiC system are related, to a large extent, to the nanoscale electro-structural properties of the interfacial region, including both the metal and the underlying implanted 4H-SiC. Hence, other experimental electrical and structural measurements (presented in the next paragraphs) were carried out in order to give a clearer physical scenario explaining our result.

3.3 Temperature dependence of the electrical properties of implanted 4H-SiC and Ti/Al Ohmic contacts

Firstly, the macroscopic electrical properties of the Al-implanted 4H-SiC (averaged over the entire implanted thickness) were monitored by means of both TLM analysis and room temperature Hall measurements.

The values of the sheet resistance R_{SH} of the implanted layer, determined by TLM analysis, are reported in Table 2. As can be seen, R_{SH} did not significantly depend on the use of the capping layer during high-temperature activation annealing, but it mainly depends on the Al-implanted dose. In fact, in the samples implanted at high dose the sheet resistance was in the order of 25 kΩ/sqr, while in the samples implanted at low dose was in the range 76-80 kΩ/sqr.

Room temperature Hall measurements allowed to estimate the free hole concentration in the implanted layer. Assuming a uniformly implanted layer of thickness t_{imp} =175 nm, free holes concentration values of 6.63×10^{17} cm^{-3} and of 6.42×10^{17} cm^{-3} were determined for the samples implanted at high dose and annealed with and without capping layer, respectively. On the other hand, in the samples implanted at low – dose hole concentration values of 1.01×10^{17} cm^{-3} and of 9.96×10^{16} cm^{-3} were found respectively for the samples annealed with and without capping layer. The values of the Hall mobility, determined using a Hall scattering factor of 0.8 [31], were in the order of 17 $cm^2V^{-1}s^{-1}$ and 37 $cm^2V^{-1}s^{-1}$ for the high and the low implantation dose, respectively. Hence, as already observed for the sheet resistance, also the mobility is not influenced by the surface morphology.

The high values of sheet resistance and low free hole concentration determined at room temperature can be associated to an incomplete activation of the implanted Al dopant atoms. In fact, the free hole concentration p is only a small fraction of the implanted concentration, due to the high energy of the acceptor levels (~190 meV) [32] or to an incomplete activation of the implanted Al [33]. As a consequence, in some devices applications, like in the case of a JBS where p-type implanted stripes are integrated inside a n-type drift region, the high sheet resistance imposes a constraint in the layout, consisting in the need of a good Ohmic metallization over the entire stripe, in order to avoid any undesired potential drop and excess of series resistance under high current operation [3].

The sheet resistance R_{SH} of the implanted layer was determined by TLM analysis as a function of the temperature, performing TLM measurements varying the sample temperature between 25°C and 150°C. The results are shown in figure 2 for the sample implanted at high dose and annealed *with* or *without* the capping layer.

In both samples R_{SH} decreases in a similar way with increasing measurement temperature T, from around 25 kΩ/sqr at room temperature to 6.6 kΩ/sqr at 425 K.

For a uniformly implanted layer of thickness t_{imp}, the temperature dependent sheet resistance $R_{SH}(T)$ is related to the free hole concentration $p(T)$ and to the holes mobility $\mu_p(T)$ by the relation:

$$R_{SH}(T) = \frac{1}{q\mu_p(T)\,p(T)t_{imp}} \tag{1}$$

where q is the elementary charge.

For a p-type semiconductor the net free hole density $p(T)$ depends both on the acceptor concentration N_A and on the concentration of compensating donor centres N_D [34]. In particular, in the examined temperature range, the temperature dependence of free hole concentration $p(T)$ can be expressed by a simplified form [27,10].

$$p(T) \approx \frac{(N_A - N_D)N_V}{gN_D}\exp\left(-\frac{E_A}{kT}\right) \tag{2}$$

where N_V is the effective density of states in the valence band, g the degeneracy factor for acceptors (usually taken as 4), k is the Boltzmann constant, T the absolute temperature and E_A the ionization energy of acceptors referred to the top of the valence band.

The mobility μ_p depends both on N_A and on the temperature T. This dependence can be described by the following relation [35]:

$$\mu_p(T, N_A) = \mu_p(300, N_A)\left(\frac{T}{300}\right)^{-\beta(N_A)} \tag{3}$$

where $\mu_p(300, N_A)$ is the mobility at T=300 K and $\beta(N_A)$ is an empirical parameter which depends on the implanted doping concentration.

Hence, using the expression of N_V [27], the literature value $\beta(N_A) = 2.56$ for our doping conditions [35], and the experimental value of $\mu_p(300, N_A)$ determined by Hall measurements, it is possible to combine the Eqs. (2) and (3) with the expression of the sheet resistance (Eq. (1)), demonstrating that R_{SH} follows a thermally activated dependence as:

$$R_{SH} = T^{1.06}\frac{gN_D}{N_A - N_D}\frac{h^3}{2(2\pi m^*)^{3/2}}\frac{300^{-\beta}}{qt_{imp}\mu_p(300, N_A)}\exp\left(\frac{E_A}{kT}\right) \tag{4}$$

Hence, reporting in a semilogarithmic plot $\frac{R_{SH}}{T^{1.06}}$ as a function of the inverse of the absolute temperature should give an Arrhenius dependence, from which the activation energy can be determined.

Figure 3 reports the semilogarithmic plot of $\frac{R_{SH}}{T^{1.06}}$ as a function of q/kT, determined from the data in figure 2, for the samples implanted at high dose and annealed with and without capping layer. As it can be seen, the experimental data follows an Arrhenius law according to Eq. (4). From a linear fit, it was possible to determine the values of the activation energy E_A of 144 meV for the sample annealed with capping layer and 141 meV for the sample annealed without capping layer.

Clearly, all the electrical results presented above provided average information on the properties of the implanted layer (like the sheet resistance, free carrier concentration, mobility activation energy of the dopant), indicating that all these macroscopic quantities are not significantly affected by the surface morphology obtained in our conditions. However, in order to get further physical insights into the properties of Ohmic contacts, namely on the current transport at the Al/Ti/SiC interface, we monitored the temperature dependence of the specific contact resistance. In fact, in a metal/semiconductor system this dependence is typically related to fundamental physical parameters, like the barrier height Φ_B and the doping density N [36]. In particular, the barrier height is extremely sensitive to the interfacial properties (like the microstructure, presence of different phases, uniformity and surface inhomogeneity of the dopant activation). Such an analysis provided interesting information to understand the different electrical behaviour of the contacts fabricated on implanted SiC annealed with or without the capping layer.

The specific contact resistance ρ_c as a function of the temperature T, for the samples implanted at high-dose (with and without capping layer) is shown in figure 4. First of all, it can be observed that the values of ρ_c for the Ti/Al Ohmic contacts formed on 4H-SiC surfaces implanted and annealed with capping layer are lower that those measured in the samples without capping layer in the entire examined temperature range. Moreover, in both cases the specific contact resistance ρ_c decreases with increasing measuring

temperatures *T*. In particular, for Ti/Al contacts formed on capped 4H-SiC surface, ρ_c decreased from 1.45×10^{-4} Ωcm^2 at room temperature to 2.49×10^{-5} Ωcm^2 at 150°C. On the other hand, for the Ti/Al contact formed on the uncapped 4H-SiC ρ_c decreased from 3.51×10^{-4} Ωcm^2 to 9.69×10^{-5} Ωcm^2 in the same temperature range.

According to the classical treatment, the dominant carrier transport mechanism in metal/semiconductor interface depends on the doping density of the semiconductor *N*, and is related to a characteristics energy E_{00} defined by [37]:

$$E_{00} = \frac{h}{4\pi}\left(\frac{N}{m^*\varepsilon}\right)^{\frac{1}{2}} \tag{5}$$

where *h* is the Planck's constant, m^* is the hole effective mass and ε the dielectric permittivity of SiC.
E_{00} gives the relationship between the temperature *T* and the semiconductor net doping ($N = N_A - N_D$). The ratio kT/qE_{00} quantifies the ratio between the thermionic emission (TE) current and other contributions like the thermionic field emission (TFE) or the field emission (FE) one. A comparison of the thermal energy *kT* with E_{00} calculated for our doping levels and temperature range leads to $kT/qE_{00} \approx 0.86 - 1$. Hence, TFE can be assumed to be the dominant carrier transport mechanism.
According to the TFE model, the specific contact resistance can be expressed as [37,38]:

$$\rho_C = \left(\frac{1}{qA^*}\right)\frac{k^2}{\sqrt{\pi(\phi_B + V_n)E_{00}}}\cosh\left(\frac{E_{00}}{kT}\right)\times\left[\sqrt{\coth\left(\frac{E_{00}}{kT}\right)}\right]\exp\left(\frac{\phi_B + V_n}{E_0} - \frac{V_n}{kT}\right) \tag{6}$$

where

$$E_0 = E_{00}\coth\left(\frac{E_{00}}{kT}\right) \tag{7}$$

In Eq. (6) A^* is the Richardson constant and V_n the energy difference between the conduction band edge and the Fermi level.

The experimental data, reported in figure 4 were fitted using the expression of the TFE model, and the Schottky barrier height Φ_B and the doping concentration *N* were considered as fit parameters. Since the experimental results showed in the previous paragraph indicated that the average electrical properties of the implanted layer are almost independent on the use of the capping layer, a reasonable physical assumption is to consider the same value of *N* for both cases. Basing on this assumption, the experimental data for the two cases were fitted simultaneously, imposing the constrain of having the same parameter *N*.
For our calculation we used the values of $\varepsilon = 9.7\varepsilon_0$, ε_0 being the permittivity of free space, $A^* = 146$ A/cm^{2}K [39], and $m^* = 0.91\ m_0$ [40], with m_0 the electron mass.
For the sample annealed with capping layer a good fit of the experimental data was obtained using the TFE model, from which the values of $N=(2.0\pm0.1)\times10^{19}$ cm^{-3} and $\Phi_B=(0.46\pm0.01)$ eV were determined.
The value of *N* determined by the fit with the TFE model, that corresponds to an electrical activation of the dopant of around 20%, is in good agreement with previous experimental measurements of Al electrical activation in 4H-SiC obtained under similar doping conditions [41].
Few works reported the experimental values of the barrier height for Ti-Al based contacts to p-type implanted 4H-SiC, and these values critically depend on the contact formation conditions (e.g., metal thickness, deposition technique, doping and annealing conditions). As an example, using temperature dependent TLM measurements Scorzoni *et al*. [42] found a value of $\Phi_B=0.82$ eV on p-type ion implanted 4H-SiC for a doping concentration of 4×10^{19} cm^{-3}, while Crofton *et al.* [43] modeled the dependence of ρ_c on N_A assuming a barrier height of 0.37 eV. None of them, however, considered the incomplete activation of implanted Al.
By applying the TFE model considering the same doping concentration *N*, also for the sample annealed without capping layer, a higher Schottky barrier height ($\Phi_B=0.51\pm0.01$) eV was determined.
On the basis of this analysis, it can be concluded that TFE is the dominant transport mechanism in our Ti/Al Ohmic contacts. Furthermore, the reduction of the specific contact resistance, observed in the sample annealed with the capping layer, can be associated to a lowering of the Schottky barrier from 0.51 eV to 0.46 eV. However, it cannot be ruled out that local differences in the electrical activation of implanted Al-ions in the near-surface region occurring when using a capping layer, observed by scanning probe microscopy measurements in the absence of metal contacts [41], can play a role in the improvement of the values of ρ_c.

Furthermore, the deviations of the experimental data from model can be associated to the presence of an inhomogeneous metal–SiC interface, not considered in the classical TFE mechanism.

3.4 Microstructure of Ti/Al Ohmic contacts

In order to explain the different electrical behavior and to corroborate the information gained from the temperature dependence of ρ_c, the microstructure of the samples was evaluated by XRD analysis combined with cross-sectional TEM investigation.

Figure 5 shows XRD patterns of Ti/Al contact after annealing at 950 °C for the sample at high dose with capping layer. The main feature that can be deduced from the XRD patterns is the formation of a ternary compound Ti_3SiC_2 and of the Al_3Ti phase and the presence of unreacted Al. The same phases were observed in the sample annealed without capping layer (not shown). The phases observed by XRD in the alloyed contacts are in agreement with the predictions of the phase diagram of the Al-C-Ti-Si quaternary system, which indicates the coexistence of Ti_3SiC_2 and other compounds (like Al_4C_3 or Al_3Ti) upon annealing at 1000°C [44]. The presence of Al_4C_3, experimentally observed by Johnson et al [22], has not been detected in our samples, probably due to different annealing conditions.

Cross section TEM analysis, allowed the evaluation of contacts microstructure in the proximity of the interface, being relevant to understand the electrical properties determined by TLM analysis. Figures 6a and 6b show the cross sectional TEM micrographs for samples implanted at high dose and annealed at 1700°C without and with a capping layer, respectively. The combination of XRD (figure 5) and Energy Filtered TEM (EFTEM) analysis (this latter not shown in this paper), allowed to identify the elemental composition of the grains inside the reacted metal layer. The brighter regions in the TEM micrographs have been generically indicated as “Al-rich regions”, since the chemical analysis showed a predominance of Al, without the possibility to rule out the presence of small amount of Ti. Hence, according to the XRD analysis, inside these regions both pure Al and Al_3Ti may coexist. Furthermore, the ternary phase Ti_3SiC_2 is observed in both samples, resulting from the interaction of Ti with SiC at such high temperatures [44]. However, while in the sample without capping layer (figure 6a), large Ti_3SiC_2 grains are located close to the interface with SiC and interrupted by small Al-rich regions, in the sample with capping layer (figure 6b), larger Al-rich regions are found, in some parts forming an almost continous interfacial layer. Large agglomerates, already observed by AFM, were visible by TEM imaging in some places on the contact surface, and can be due to an excess of liquid Al freezed when cooling down the samples after annealing. Below the metal/SiC interface, a high density of extended defects can be observed, which was likely formed as a result the high dose implant followed by high temperature annealing. The presence of these defects is one of the causes of the high sheet resistance measured in the implanted material.

Evidently, TEM analysis showed a strongly inhomogeneous interface, where the interfacial morphology and microstructure are affected by the roughness of the implanted SiC. Although Ti was originally in contact with SiC, annealing of the contacts resulted in the formation of Ti_3SiC_2 interrupted by Al-rich regions. On the other hand, Tsukimoto *et al.* [26] found an irregular surface and interface morphology of the annealed Ti/Al system, attributing them to an anisotropic growth process of hetero-epitaxial Ti_3SiC_2 layers onto off-axis SiC layers. However, the ternary phase totally covered the area of the SiC substrate in their case. An inhomogeneous interfacial microstructure, similar to that of our samples, was found also by Parisini *et al.* [45], who detected the presence of titanium compounds and Al or Al_3Ti agglomerates, but did not report any correlation with the electrical measurements.

4. Summary

In summary, the carrier transport mechanism in alloyed Ti/Al Ohmic contacts to p-type Al-implanted 4H-SiC was modelled in this work considering transport mechanism at inomogeneous interfaces. It has been shown that the morphology of implanted SiC after high temperature (1700°C) annealing strongly influences both the surface flatness and the electrical characteristics of alloyed Al/Ti Ohmic contacts formed on it. In particular, improving the SiC surface morphology using a protective cap during post-implantation annealing resulted in a reduction of the roughness even if a uniform interface, similar to epitaxial substrates, cannot be achieved. Anyway a lowering of the specific resistance ρ_c of alloyed Ti/Al Ohmic contacts was achieved.This result could not be correlated to macroscopic electrical properties of the implanted layer, that

were independent on the surface conditions. However, the temperature dependence of the ρ_c indicated that thermionic field emission is the dominant transport mechanism through the metal/SiC interface, and that a reduction of the barrier height occurs in the contacts formed on smoother SiC surface and explains the lower specific contact resistance. As a matter of fact, TEM analysis shows an inhomogenous interface, different in the two cases, which can justify the different macroscopically measured Schottky barrier heights.

The practical implications of an improved Ohmic contact morphology and specific contact resistance, with respect to the possible applications to SiC device processing and performances were discussed.

Acknowledgements

The authors would like to thank L. Romano for help and discussion concerning Hall measurements, and K. Zekentes for the fruitful discussion during ECSCRM2010 in Oslo. C. Bongiorno and S. Di Franco are greatly acknowledged for TEM analysis and for samples processing, respectively.
This work was supported by ST Microelectronics of Catania and by the LAST POWER project. The LAST POWER project has received funding from the ENIAC Joint Undertaking under grant agreement n° 120218 and from the national programmes/funding authorities of Greece, Italy, Poland, and Sweden.

Table 1. Surface roughness (RMS) of 4H-SiC and alloyed Ti/Al contacts for the different implantation/annealing conditions.

	High – dose		**Low – dose**	
as–grown 4H-SiC	0.9 nm		0.9 nm	
as-implanted 4H-SiC	1.14 nm		1.10 nm	
	Without Cap	**With Cap**	**Without Cap**	**With Cap**
Implanted and annealed (1700°C) 4H–SiC	18.9 nm	2.4 nm	9.0 nm	1.3 nm
Alloyed (950°C) Ti/Al contacts	44.0 nm	22.8 nm	43.5 nm	20.8 nm

Table 2. Specific contact resistance ρ_c of alloyed Ti/Al contacts and sheet resistance R_{SH} of Al-implanted 4H-SiC measured at room temperature for the different implantation/annealing conditions.

	With cap		**Without cap**	
	High-dose	**Low-dose**	**High-dose**	**Low-dose**
$\rho_C(\Omega cm^2)$	1.45×10^{-4}	7.52×10^{-4}	3.51×10^{-4}	3.70×10^{-3}
$R_{SH}(\Omega/sqr)$	24.84×10^{3}	76.56×10^{3}	25.45×10^{3}	80.50×10^{3}

FIGURE CAPTIONS

Figure 1. AFM scans of Al-implanted 4H-SiC surface for samples implanted at high-dose and annealed at 1700°C without capping layer (a) and with capping layer (b). AFM scans of alloyed Ti/Al contacts formed on Al-implanted 4H-SiC surface for samples annealed without capping layer (c) and with capping layer (d).

Figure 2. Sheet resistance R_{SH} of implanted 4H-SiC as a function of the measurement temperature for the high implantation dose and annealing at 1700°C "with" and "without" capping layer.

Figure 3. Semilogarithmic plot of $\frac{R_{SH}}{T^{1.06}}$ as a function of *q/kT* for the samples implanted at high-dose and annealed at 1700°C "with" and "without" capping layer.

Figure 4. Specific contact resistance ρ_c as a function of the measurement temperature for alloyed Ti/Al contacts formed on 4H-SiC implanted at high-dose and annealed at 1700°C "with" and "without" capping layer. The fits obtained using TFE model for the both samples implanted at high dose and annealed at 1700 °C "with" and "without" protective capping layer are also reported.

Figure 5. XRD analysis of a Ti/Al contact after annealing at 950 °C formed on implanted 4H-SiC

Figure 6. Cross sectional TEM micrographs of the interfacial region for samples implanted at high dose and annealed at 1700°C "without" capping layer (a) and "with" capping layer (b).

References

[1] Pensl G, Ciobanu F, Frank T, Krieger M, Reshanov S, Schmid F and Weidner M 2006 *SiC Materials and Devices,* Shur M, Rumyanstev S and Levinshtein M eds., Singapore, World Scientific, Vol. 1, pag. 1-41.
[2] Roccaforte F, Giannazzo F, Raineri V 2010 *J. Phys. D: Appl. Phys.* **43** 223001.
[3] Baliga BJ 2005 *Silicon Carbide Power Devices*, Singapore, World Scientific.
[4] Mitra S, Rao M V, Papanicolaou N, Jones K A, Holland O W, Vispute R D, Wilson SR 2004 *J. Appl. Phys*. **95** 69.
[5] Roccaforte F, Libertino S, Giannazzo F, Bongiorno C, La Via F, Raineri V 2005 *J. Appl. Phys* **97** 123502.
[6] Laube M, Schmid F, Pensl G, Wagner G, Linnarsson M, Maier M 2002 *J. Appl. Phys.* **92** 549.
[7] Saks N S*,* Agarwal A K*,* Ryu S-H, and Palmour J W 2001 *J. Appl. Phys.* **90** 2796.
[8] Negoro Y, Kimoto T, Matsunami H, Schmid F and Pensl G 2004 *J. Appl. Phys.* **95** 4916.
[9] Sundaresan S G, et al., 2008 *Solid-State Electronics* **52** 140.
[13] Rambach M, Bauer A J, and Ryssel H 2008 *Phys. Stat. Sol. (b)* **245** (7) 1315.
[14] Brauer G, Anwand W, SkorupaW, Brandstetter S and Teichert C, 2006 *J. Appl. Phys.* **99** 023523.
[15] Giannazzo F, Rambach M, Salinas D, Roccaforte F and Raineri V 2009 *Mater. Sci. Forum* **615-617** 457.
[16] Vassilevski K V, Wright N G, Horsfall A B, O'Neill A G, Uren M J, Hilton K P, Masterton A G, Hydes A J and Johnson C M 2005 *Semicond. Sci. Technol*. **20** 271.
[17] Nipoti R, Mancarella F, Moscatelli F, Rizzoli R, Zampolli S, Ferri M 2010 *Electrochem. Solid-State Lett.* **13** H432.
[18] Crofton J, Money S E, Williams J R, Isaacs-Smith T 2002 *Solid-State Electronics* **46** 109.
[19] Roccaforte F, La Via F, Raineri V 2005 *Int. J. High Speed Electronics and Systems* **15** 781.
[20] Tsukimoto S, Sakai T, Onishi T, Ito K, and Murakami M, 2005 *J. Electronic Materials* **34** 1310.
[21] Moscatelli F, Scorzoni A, Poggi A, Cardinali GC, Nipoti R 2003 *Semicond. Sci. Technol.* **18** 554.
[22] Johnson B J, Capano M A 2004 *J. Appl. Phys.* **95** 5616.
[23] Wang Z, Saito M, Tsukimoto S, and Ikuhara Y 2009 *Advaced Materials* **21** 4966.
[24] Mohney S E, Hull B A, Lin J Y, Crofton J 2002 *Solid-State Electronics* **46** 689.
[25] Kolaklieva L, Kakanakov R, Avramova I, Marinova Ts 2007 *Mater. Sci. Forum* **556-557** 725.
[26] Tsukimoto S, Ito K, Wang Z, Saito M, Ikuhara Y, Murakami M 2009 *Materials Transactions* **50** 1071.
[27] Schroder D K 2006 *Semiconductors Materials and Device Characterization*, 3rd ed., New York, John Wiley & Sons, p. 135.
[28] La Via F, Galvagno G, Roccaforte F, Ruggiero A, Calcagno L, 2005 *Appl. Phys. Lett.* **87**, 142105.
[29] Ito K, Tsukimoto S, Murakami M 2006 *Science and Technology of Advanced Materials* **7** 496.
[30] Tsao B H, Liu S, Scofield J 2004 *Mater. Sci. Forum* **457-460** 841.
[31] Pensl G, Schmid F, Ciobanu F, Laube M, Reshanov S A, Schulze N, Semmelroth K, Nagasawa H, Schöner A, Wagner G 2003 *Mater. Sci. Forum* **433 – 436** 365.
[32] Pernot J, Contreras S, Camassel J 2005 *J. Appl. Phys.* **98** 023706.
[33] Giannazzo F, Roccaforte F, Raineri V 2007 *Appl. Phys. Lett.* **91** 202104.
[34] Sze S M, 2001 *Semiconductor Devices: Physics and Technology*, 2nd ed., New York, John Wiley & Sons Inc.
[35] Matsuura H, Komeda M, Kagamihara S, Iwata H, Ishihara R, Hatakeyama T, Watanabe T, Kojima K, Shinohe T, Arai K 2004 *J. Appl. Phys.,* **96** 2708.
[36] Iucolano F, Roccaforte F, Alberti A, Buongiorno C, Di Franco S, Raineri V 2006 *J. Appl. Phys.* **100** 123706.
[37] Padovani F A, Stratton R 1966 *Solid – State Electron* **9** 695.
[38] Yu A Y C 1970 *Solid-State Electronics* **13** 239.
[39] Roccaforte F, La Via F, Raineri V, Pierobon R, Zanoni E 2003 *J. Appl. Phys.* **93** 9137.
[40] Son N T, Hai P N, Chen W M, Hallin C, Monemar B, Janzén E 2000 *Phys. Rev. B* **61** R10544.
[41] Weng M H, Roccaforte F, Giannazzo F, Di Franco S, Bongiorno C, Saggio M, Raineri V 2010 *Mater. Sci. Forum* **645-648** 713.
[42] Scorzoni A, Moscatelli F, Poggi A, Cardinali G C, Nipoti R 2004 *Mater. Sci. Forum* **457-460** 881.
[43] Crofton J, Porter L M, Williams J R 1997 *Phys. Stat. Sol. (b)* **202** 549.
[44] Viala J C, Peillon N, Bosselet F, Bouix J 1997 *Mat. Sci. Eng.,* **A229** 95.
[45] Parisini A, Poggi A, Nipoti R 2004 *Mater. Sci. Forum* **457-460** 837.

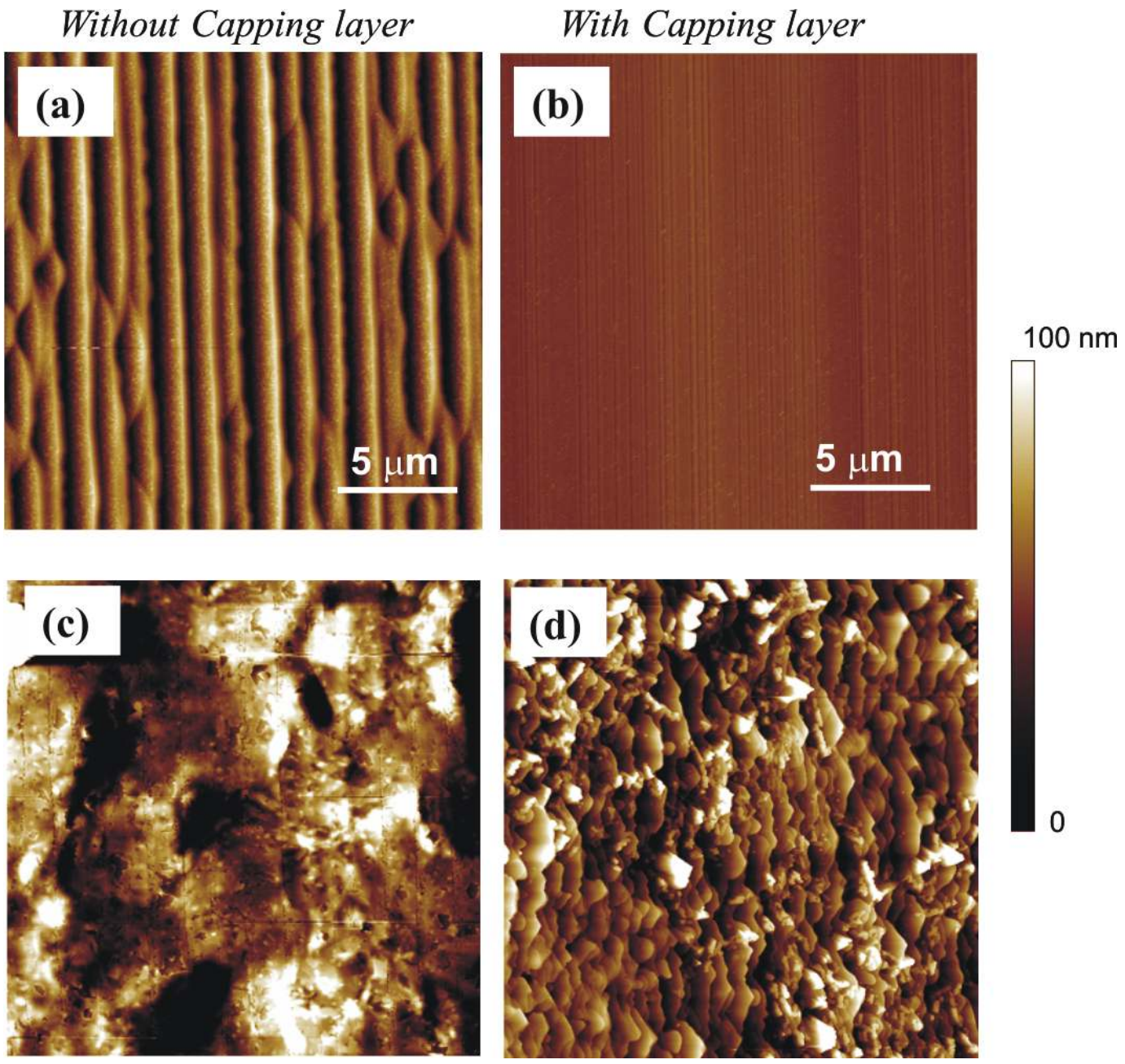

Figure 1 (Figure1.tif)

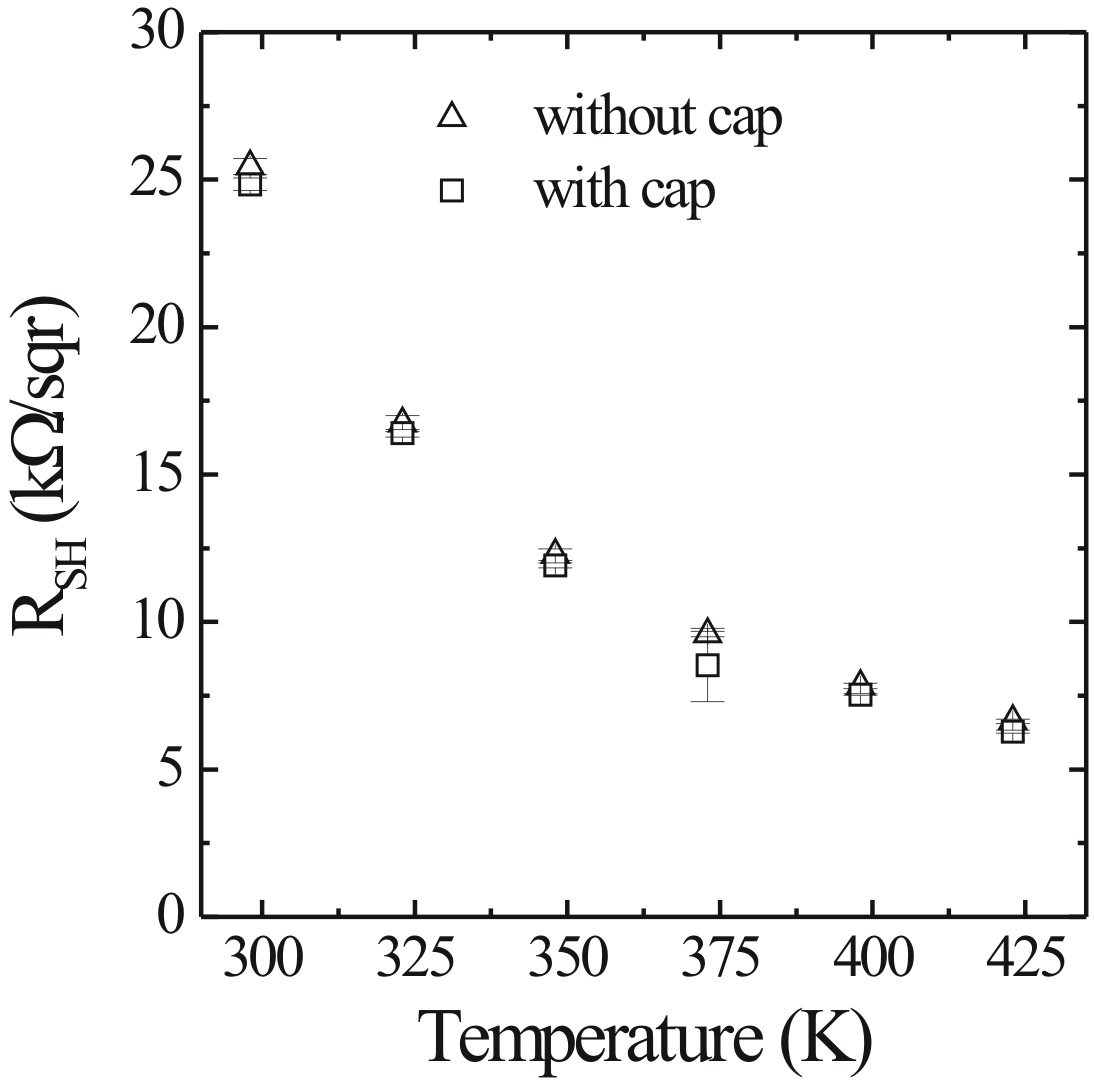

Figure 2 (Figure2.tif)

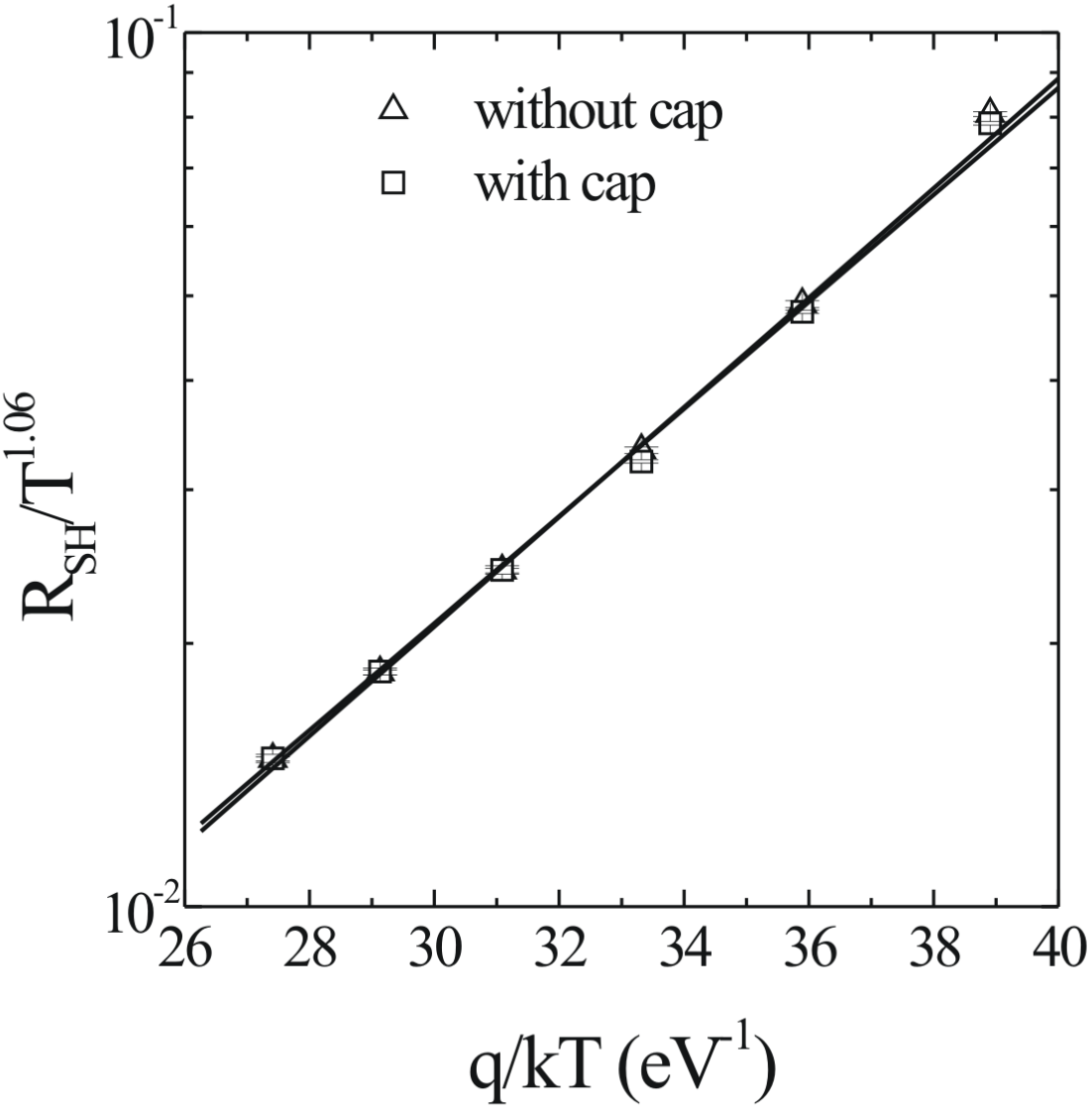

Figure 3 (Figure3.tif)

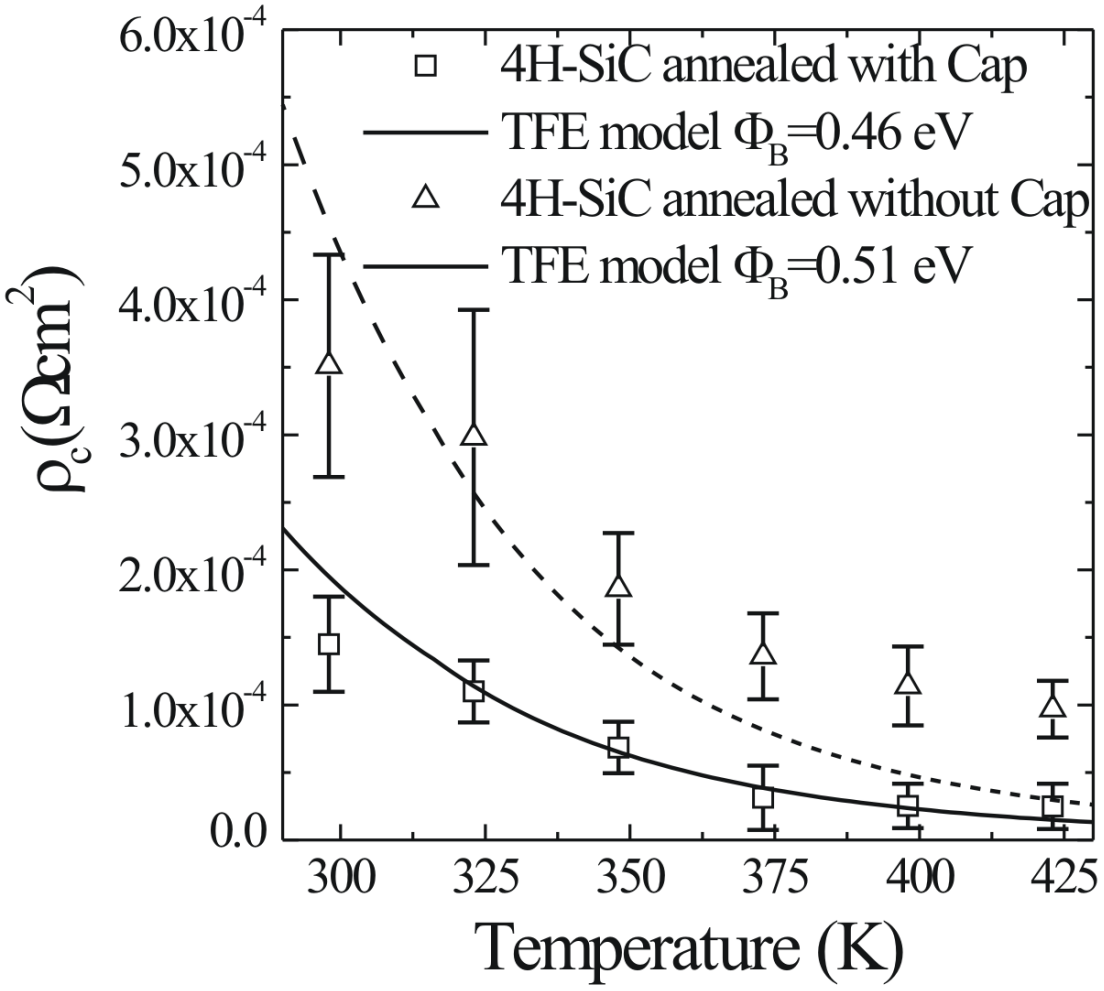

Figure 4 (Figure4.tif)

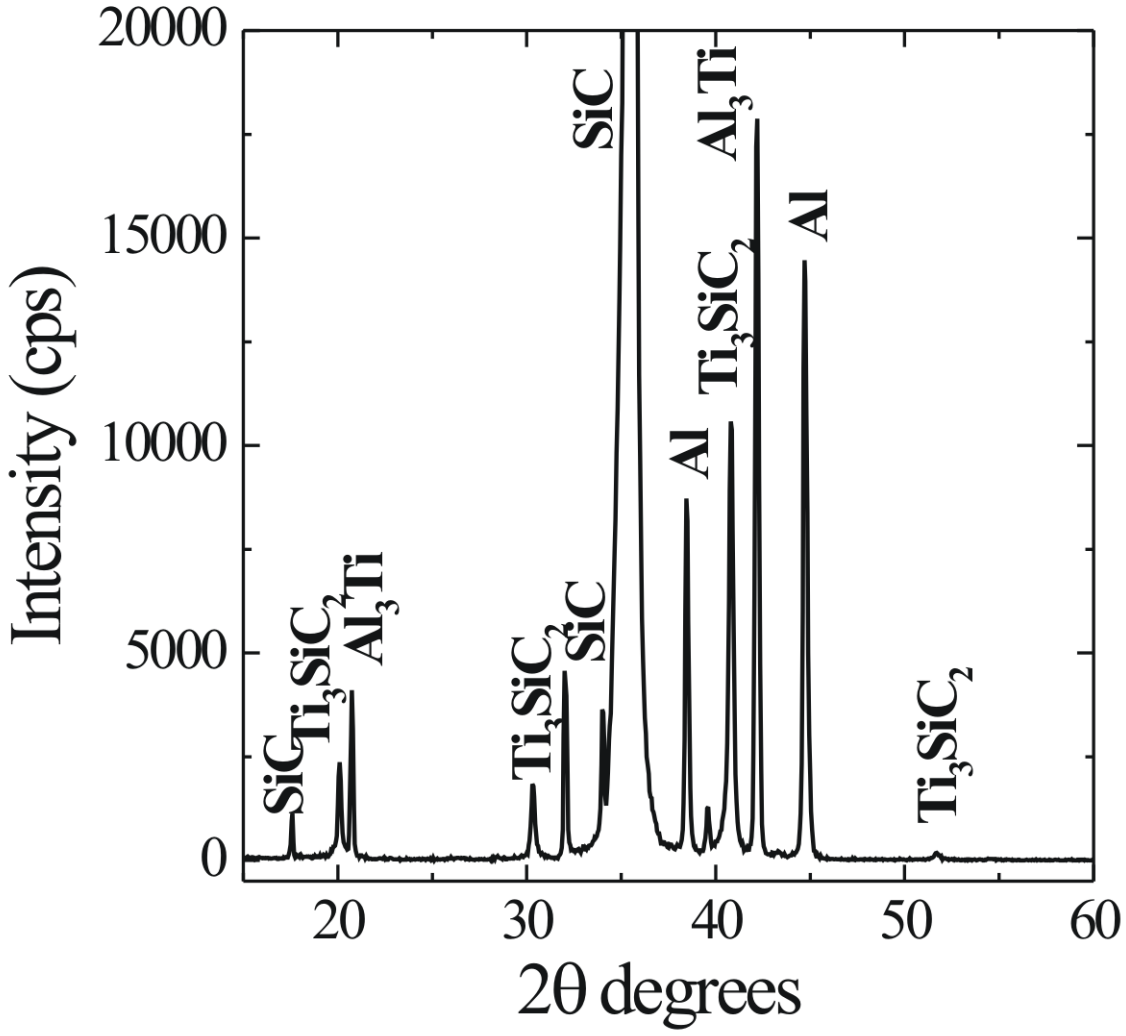

Figure 5 (Figure5.tif)

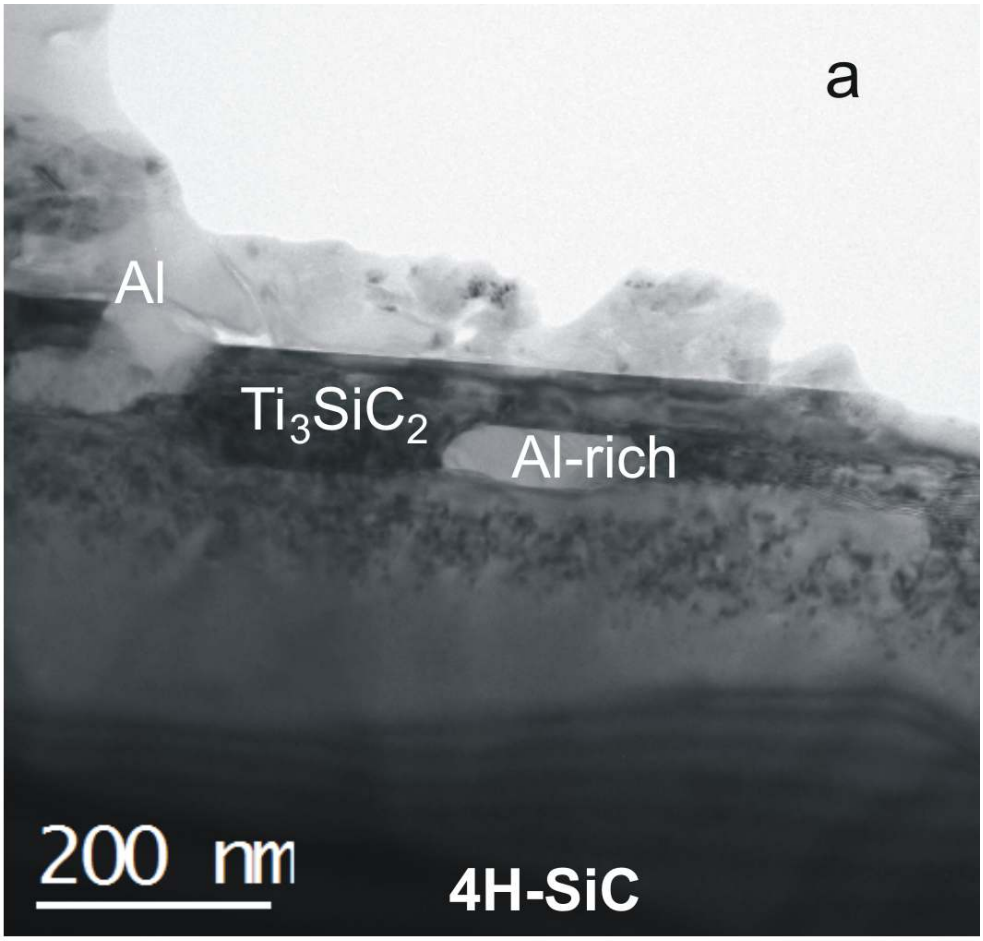

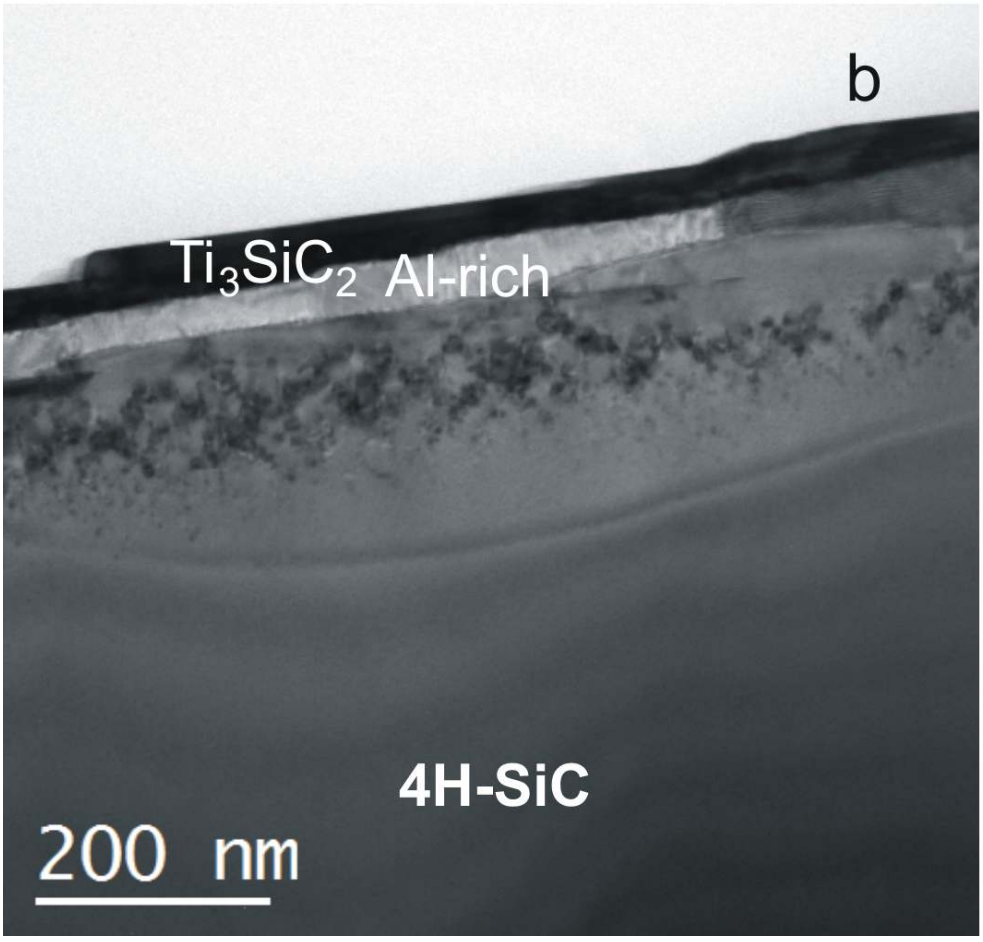

Figure 6 (Figure6.tif)